Science of the Total Environment 806 (2022) 150456

Contents lists available at ScienceDirect

Science of the Total Environment

journal homepage: www.elsevier.com/locate/scitotenv

Elevated levels of radiocarbon in methane dissolved in seawater reveal likely local contamination from nuclear powered vessels

DongJoo Joung [a,*,1], Carolyn Ruppel [b], John Southon [c], John D. Kessler [a]

[a] Department of Earth and Environmental Sciences, University of Rochester, 227 Hutchison Hall, P.O. Box 270221, Rochester, NY 14627, USA
[b] U.S. Geological Survey, 384 Woods Hole Rd. Woods Hole, MA 02543, USA
[c] Earth System Science Department, University of California, Irvine, 215 Aldrich Hall, Irvine, CA 92697, USA

HIGHLIGHTS

- ^{14}C analysis in CH_4 dissolved in seawater was conducted to constrain CH_4 dynamics.
- Extremely high ^{14}C-CH_4 values were observed in some water samples.
- Emission of the $^{14}CH_4$ isotopologue from nuclear-powered vessels is likely the cause.
- This source can alter geoscience results and regionally trace vessel positions.

GRAPHIC ABSTRACT

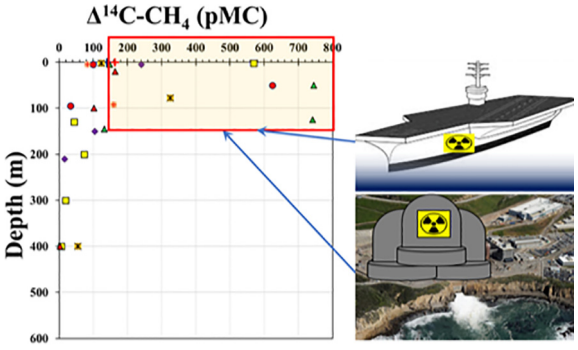

ARTICLE INFO

Article history:
Received 15 July 2021
Received in revised form 14 September 2021
Accepted 15 September 2021
Available online 21 September 2021

Editor: Jay Gan

Keywords:
Methane isotopologue
^{14}C-CH_4
Nuclear power
Atlantic Ocean
Pacific Ocean

ABSTRACT

Measurements of the natural radiocarbon content of methane (^{14}C-CH_4) dissolved in seawater and freshwater have been used to investigate sources and dynamics of methane. However, during investigations along the Atlantic, Pacific, and Arctic Ocean Margins of the United States, as well as in the North American Great Lakes, some samples revealed highly elevated ^{14}C-CH_4 values, as much as 4–5 times above contemporary atmospheric ^{14}C-CH_4 levels. Natural production of the $^{14}CH_4$ isotopologue is too low to cause these observations nor can it explain the variations in location and depth. Numerous lab and field validation tests and blanks, as well as the relatively small number of samples that display these elevated values, all suggest that these signals are not derived from an unknown procedural issue. Here we suggest that the byproducts of nuclear power generation include localized discharges of the $^{14}CH_4$ isotopologue into marine and aquatic environments, severely altering the measured ^{14}C-CH_4 isotopic signals. Since several of our sample sites are distant from on-land nuclear powerplants, we conduct further calculations concluding that the most elevated anomalies in ^{14}C-CH_4 likely originate with discharge from nuclear-powered vessels.

1. Introduction

Methane (CH_4) is a potent greenhouse gas that contributes significantly to contemporary atmospheric warming trends (Saunois et al., 2016). Atmospheric CH_4 concentrations have more than doubled over the industrial era and are predicted to continue rapidly increasing due to intense production of oil and natural gas,

* Corresponding author.
E-mail address: djjoung@snu.ac.kr (D. Joung).
[1] Current address: Research Institute of Oceanography, Seoul National University, 1 Gwanak-ro Gwanak-gu Seoul 08856 Korea (Republic of).

https://doi.org/10.1016/j.scitotenv.2021.150456
0048-9697/

agricultural activities, and positive feedbacks associated with a warming climate (Saunois et al., 2016; Brandt et al., 2014; Bruhwiler et al., 2017; Anthony et al., 2012). Ocean and freshwater environments are enormous natural reservoirs of CH_4 originating from diverse sources, many of which are expected to become stronger with warming and other anthropogenic activities (e.g. Reeburgh, 2007; Repeta et al., 2016; Ruppel and Kessler, 2017).

Different sources of CH_4 often have unique isotopic signatures, rendering natural isotopic measurements of CH_4 useful for constraining CH_4 sources in various environments (e.g. Graven, 2015). Since isotopes of one molecule can experience relative abundance changes with processes such as oxidation and dissolution (e.g. Leonte et al., 2017, 2018), natural radiocarbon analyses are particularly useful for identifying sources, since they can be precisely measured by accelerator mass spectrometry (AMS) (Muller, 2010) and normalized to remove such fractionation (Stuiver and Polach, 1977). In general, geological sources of CH_4 (also referred to as "fossil" or "dead") have ^{14}C below the detection limit because the carbon has not been exchanged with the atmosphere for longer than approximately 60,000 years or about ten ^{14}C half-lives. Such CH_4 has a radiocarbon value of 0% Modern Carbon (pMC). Studies have shown 0 pMC to be generally associated with gas hydrates, thawing permafrost, seeps, and vents (Anthony et al., 2012; Stuiver and Polach, 1977; Winckler et al., 2002; Pohlman et al., 2009; Kessler et al., 2005, 2006; Douglas et al., 2016). In contrast, more modern values of ^{14}C-CH_4 are usually observed when modern carbon is converted to CH_4, often through biological processes (e.g. Kessler et al., 2008; Sparrow et al., 2018). "Modern" ^{14}C-CH_4 (equivalent to 100 pMC) is defined as the 95% radiocarbon levels in the ^{14}C-activity in the Oxalic Acid I standard produced in year 1950, which contained no anthropogenic ^{14}C derived from nuclear bomb tests (Stuiver and Polach, 1977). Generally, CH_4 formed in the water column and in relatively shallow sediments (0–50 cm) is likely to contain more modern levels of radiocarbon (Kessler et al., 2005, 2008; Sparrow et al., 2018). Thus, ^{14}C analysis of CH_4 can identify the fractions of ancient to modern sources of this greenhouse gas, and aquatic environments with mixtures of these two endmembers can be deconvolved using CH_4 isotopic mass balances (e.g. Sparrow et al., 2018).

Current atmospheric ^{14}C-CH_4 levels are elevated relative to the "modern" definition of ^{14}C, with a value of approximately 135 pMC due to the release of the $^{14}CH_4$ isotopologue from anthropogenic nuclear activities (Lassey et al., 2007). However, the atmospheric ^{14}C-CH_4 trend changes with changing emissions from nuclear and fossil fuel activities (Graven et al., 2019). For example, the ^{14}C released from nuclear power plants (NPP) increased the $^{14}C/C$ ratio of CH_4 for the period from 1960 and 1980 to 165 pMC, and the values have since decreased due to the 1963 ban on atmospheric nuclear bomb testing and reduced use of NPPs (Lassey et al., 2007; Quay et al., 1999). Production of ^{14}C occurs through nuclear reactions with the parent isotopes ^{14}N, ^{17}O, and ^{13}C in the nuclear fuel, coolant, and structural material of nuclear reactors (Yim and Caron, 2006). The production and release of ^{14}C from NPPs depends on the type of reactor used, whether pressurized water reactors (PWRs) or boiling water reactors (BWRs) (Zazzeri et al., 2018). In PWRs, which are the most common type of NPP in use today, gaseous ^{14}C effluents are mostly in the molecular form of $^{14}CH_4$ (70–95%, Kunz, 1985) due to the reducing chemical environment of the reactor coolant. However, in all other nuclear reactor types, the gaseous ^{14}C effluent is almost entirely $^{14}CO_2$ (Zazzeri et al., 2018).

NPPs may influence ^{14}C-CH_4 measurements in some aquatic environments. Kessler et al. (2008) found ~350 pMC of ^{14}C-CH_4 in waters from Santa Barbara Basin, California, USA, close to where Joung et al. (2020) measured elevated values (~163 pMC). In addition, Joung et al. (2019) reported slightly elevated ^{14}C-CH_4 values (~145 pMC) in Lake Michigan, USA. These studies suggested that the elevated values were likely associated with NPPs located along coastlines near the sampling sites. In a coastal arctic setting, Sapart et al. (2017) also attributed extremely elevated values of ^{14}C-CH_4 to anthropogenic nuclear contamination. However, due to a lack of procedural details, the anomalous measurements could not be unequivocally traced to the natural environment instead of an unknown analytical issue during sample collection, preparation, and analysis, as noted by Sparrow and Kessler (2018).

This manuscript presents a collection of highly elevated ^{14}C-CH_4 values, >140 pMC, observed sporadically in the analysis of 84 water samples collected from oceans and Great Lakes of varying depths and distances from land (Fig. 1). We investigate natural and anthropogenic processes that could produce such high pMC values and discuss the implications of these findings for geoscientific analyses and operations of nuclear-powered vessels.

2. Materials and methods

Detailed descriptions of the data, the procedures, and the equipment for sample collection at sea and preparation for analysis in the shore-based laboratory can be found in the Supplementary Materials and Sparrow and Kessler (2017). Briefly, for the at-sea sample collections, seawater was pumped from a targeted water depth to the deck of the ship using a discharge pump. Multiple suction hoses, each 10 m in length and 7.6 cm in diameter, were connected together using cam-and-groove hose couplings and attached to the ship's winch cable using metal hose clamps to sample water at the targeted depth (Supplementary Fig. S1). The pumped water was passed through a high-performance, gas-permeable membrane filter on the deck of the ship for the vacuum extraction of the dissolved gases. To collect an adequate mass of dissolved CH_4 for a conventional ^{14}C analysis (~200 μg-C in CH_4), we extracted the dissolved gas from 21,000 to 42,000 L of seawater per sample (Table 1). The extracted gases were collected in a plastic bag (~400 L capacity) attached to the end of extraction system. Finally, the extracted gases in the plastic bag were pressurized into small (1.6 L) aluminum cylinders using a non-oil-based compressor pump for transfer back to the shore-based laboratory (Supplementary Fig. S1).

In the laboratory, the small cylinder brought from the field was connected to a glass gas purification vacuum line. Through multiple Liquid Nitrogen (LN_2) traps and ovens, this overall system isolates CH_4 from other carbon species and converts it to CO_2 and H_2O. First, the gases in

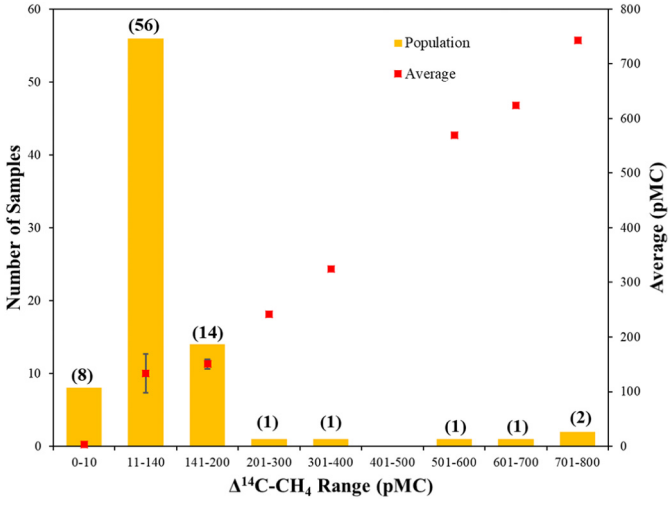

Fig. 1. 84 natural water samples from oceans (U.S. Atlantic, Pacific, and Arctic margins) and the U.S. Great Lakes were collected and analyzed using previously published procedures (40). The number of samples (orange bars, left scale) in each pMC interval and the average values of pMC (red squares, right scale) in those samples are depicted here. The contemporary atmosphere has ~135 pMC. (For interpretation of the references to colour in this figure legend, the reader is referred to the web version of this article.)

Table 1
Detailed information of samples collected from US-Atlantic and US-Pacific Margins.

	Latitude	Longitude	Date	Depth (m)	Sample Depth (m)	Temp [°C]	Salinity	DO[b] [μmol/l]	Water (L)	CH_4 (nM)	$\Delta^{14}C$-CH_4 (pMC)			$\Delta^{14}C$ (‰)			^{14}C age (BP)
US-Atlantic Margins (2017)																	
T3S3	35.532	−74.826	9/1	446	2	23.0	32.5	215	35,922	4.6	569.5	±	0.9	4695	±	7.1	Modern
					50	13.9	33.1	220		16.5							
					100	10.0	33.0	217		37.5							
					130	10.0	33.3	213	33,626	47.3	43.8	±	0.1	−562.4	±	1.2	6640
					160	14.7	35.8	159		68.2							
					200	13.0	35.6	172	27,376	74.0	73.3	±	0.1	−266.8	±	0.4	2495
					250	11.2	35.4	138		40.3							
					300	9.9	35.3	132	30,058	54.7	19.4	±	0.1	−806.5	±	3.0	13,195
					350	8.8	35.2	139		35.6							
					400	7.9	35.1	154	21,817	44.2	6.9	±	0.1	−930.8	±	10.0	21,450
					450	6.4	35.1	192		26.1							
					460	6.4	35.1	191		28.3							
T6S1	37.071	−74.661	9/3	557	2	21.7	32.2	227	34,300	3.7	123.4	±	0.2	234.0	±	0.4	Modern
					78	10.3	33.6	233	27,701	168.6	324.8	±	0.5	2248.0	±	3.2	Modern
					100	12.4	35.3	194		34.1							
					150	12.5	35.4	187		24.2							
					200	12.5	35.5	110		5.5							
					250	11.2	35.4	158		15.4							
					300	10.2	35.3	146		14.7							
					360	8.8	35.2	156		17.5							
					400	7.2	35.1	181	25,948	17.5	55.0	±	0.1	−449.5	±	0.7	4795
					450	6.2	35.1	203		20.0							
					500	5.5	35.0	220		24.0							
					520	5.5	35.0	222		23.1							
T7S1	37.113	−74.528	9/5	575	1.5	22.0	32.4	229		3.5							
					20	18.2	33.4	251	25,953	4.9	163.6	±	0.2	636.4	±	1	Modern
					50	10.2	33.7	234		11.4							
					100	12.9	35.4	199	25,955	23.5	101.6	±	0.1	15.6	±	0.0	Modern
					150	12.6	35.5	183		28.7							
					200	12.0	35.5	161		4.0							
					250	10.8	35.4	134		3.1							
					300	9.5	35.2	134		3.1							
					350	8.5	35.2	147		19.9							
					400	7.1	35.1	176	25,961	59.5	2.5	±	0.1	−974.8	±	24.3	29,580
					450	6.3	35.1	198		66.3							
					484	5.9	35.1	208		46.9							
US-Pacific Margin (2019)																	
RC -2	46.832	−124.567	5/29	103	5	13.2	30.2	309	32,428	7.7	99.2	±	0.2	−7.6	±	2.2	60
					50	8.5	33.3	137	28,319	29.9	623.9	±	1.4	5239.3	±	14.3	Modern
					93	7.6	33.9	86	42,072	68.4	33.4	±	0.1	−665.8	±	1.1	8805
RC-3	46.970	−124.934	6/5	167	5	13.3	31.7	238	33,818	4.1	147.9	±	0.3	479.2	±	3.4	Modern
					50	8.9	32.6	276	31,050	4.9	745.2	±	1.8	6451.6	±	17.7	Modern
					125	7.9	33.8	110	37,987	26.9	741.5	±	1.8	6415.4	±	17.5	Modern
					155	7.7	33.8	103	38,354	32.1	131.8	±	0.3	317.5	±	2.9	Modern
RC-4	47.585	−125.060	6/6	226	1.2	12.7	32.2	297	39,060	3.7	241.2	±	0.6	1411.9	±	3.3	Modern
					150	7.7	33.9	116	40,950	26.9	104.4	±	0.2	44.2	±	0.1	Modern
					210	6.7	34.0	86	23,142	113.8	16.2	±	0.1	−837.9	±	4.3	14,615
RC_BKG	47.247	−124.690	6/5	103	5	13.0	31.7	322	41,423	8.2	83.4	±	0.2	−166.3	±	0.4	1460
					92	6.9	34.0	87	28,578	7.7	159.7	±	0.4	597.3	±	1.3	Modern
RC-U_2	45.820	−124.033	5/30	70	0	13.8	28.8	288	21,268	10.7	140.8	±	0.3	408.1	±	0.9	Modern
RC-U_3	45.259	−124.006	5/30	18	0	11.2	35.9	202	24,844	9.0	163.5	±	0.4	635.3	±	1.8	Modern
Standards (n = 13)			2017/2019								0.3	±	0.0	−997	±	2	47,534
Field Gas Blank (n = 4)[a]			9/1/2017								99.9	±	0.7	−1.4	±	7.0	10

[a] Four field blank samples were combined after laboratory purification and combustion so that sufficient C mass was available for a ^{14}C-CH_4 analysis. Combined concentration of carbon from CH_4 in these four field background samples was 19 μg C.
[b] Dissolved Oxygen concentration.

the cylinder were passed through a molecular sieve and a LN_2 trap to remove CO_2 and non-methane hydrocarbons. Then, the gases were introduced to an oven (450 °C) to convert CO to CO_2, and this CO_2 was removed by passing through another LN_2 trap. Finally, the remaining CH_4 was converted to CO_2 through a second oven (900 °C), and the converted CO_2 was trapped on a third LN_2 trap (Supplementary Fig. S1). This CO_2 was then transferred to an acid-cleaned and pre-combusted Pyrex tube and flame sealed. These prepared samples were sent to the Keck Carbon Cycle Accelerator Mass Spectrometer (AMS) facility at UC Irvine where the ^{14}C-CH_4 and $\delta^{13}C$-CH_4 values were determined by AMS and isotope ratio mass spectrometry (IRMS), respectively.

At sea and laboratory procedures for ^{14}C-CH_4 measurements were thoroughly evaluated in Sparrow and Kessler (2017), and these procedures were closely followed throughout this study to ensure no degradation in performance. In addition, the laboratory procedures that purify and combust the extracted CH_4 samples were routinely validated by processing standard gases of high and low concentrations, as well as ultra-high purity (UHP) zero-air. The standards contained CO_2, CO, and CH_4 customized to encompass the concentration ranges determined in the sample cylinders. These gas standards were analyzed after every 4–5 natural samples were processed (Supplementary Fig. S2). The purification and combustion efficiencies and total C blanks were also checked (see, Supplementary Materials for details).

Discrete bottle samples to determine the dissolved CH_4 concentration were also collected at the same sites as the ^{14}C-CH_4 samples. The concentration of CH_4 was determined using an Agilent 6850 gas chromatograph with a flame ionization detector (GC-FID) using procedures previously described in Weinstein et al. (2016) and Leonte et al. (2017).

3. Results and discussion

Of the total 84 sample set, most samples (56 out of 84) were in the range of 10–140 pMC for ^{14}C-CH_4, and 8 samples were below 10 pMC (Fig. 1). These results can all be explained by natural variations. However, 20 out of the 84 samples were higher than 140 pMC; 16 of these 'elevated' samples were in the range of 140–350 pMC and the remaining 4 samples were within the range of 570–745 pMC. In this paper we focus the discussion on the highest values (>140 pMC) observed in the U.S. Atlantic Margin (USAM) and U.S. Pacific Margin (USPM) samples (Fig. 2).

Three sites on the USAM upper continental slope between Chesapeake Bay and Cape Hatteras had elevated ^{14}C-CH_4 values at shallow water depths (569.5 and 163.6 pMC in the surface waters at station T3S3 and T7S1, respectively, and 324.8 pMC at 80 m depth at station T6S1). Other samples collected at different depths at the same sites had ^{14}C-CH_4 lower than contemporary values (Fig. 3 and Table 1). On the USPM, two sites (stations RC-S2 and RC-S3) offshore Washington displayed extremely high ^{14}C-CH_4 values of 623.9–745.2 pMC at water depths of 50–125 m, while the surface water samples at stations RC-S4, RC-U2, and RC-U3, and the bottom water sample (92 m) at station RC-BKG offshore Washington and Oregon all had significantly elevated values of ^{14}C-CH_4 (241.8, 140.8, 163.5, and 159.7 pMC, respectively). Other water depths at these USPM sites did not have anomalously high ^{14}C-CH_4 (Fig. 3).

Below, we comprehensively investigate the processes that could cause high ^{14}C-CH_4 values. These processes include (1) potential contamination or isotopic alteration associated with the sample collection and purification procedures; (2) natural production by cosmic ray spallation reactions; (3) natural methanogenesis and natural isotopic fractionation; and (4) discharges from NPPs and/or nuclear-powered vessels near the sampling sites close to the time of sample collections.

3.1. Unlikely causes of anomalous values of ^{14}C-CH_4

3.1.1. Analytical procedures

Previous experiments have used trace injections of the $^{14}CH_4$ isotopologue to determine rates of aerobic CH_4 oxidation (e.g., Pack et al., 2011 and references therein). One possible explanation for our anomalous results is that contamination from these previous experiments on either the research vessel or in the land-based laboratory influenced our results. However, no such experiments were conducted during our research cruises, and our laboratory has no history of using this isotopologue. In addition, field gas blank tests were conducted during the USAM sampling campaign using UHP zero-air to check any residual and ambient gas contaminations during compression and sample handling. For the four field blank tests conducted, the total combined blank mass was 19 μg-C, which, per sample, is <2% of our typical C mass collected (~250 μg-C in CH_4, Supplementary Table S1). The ^{14}C-CH_4 of the total blank was ~100 pMC (Table 1), which indicates that our analytical procedures are not the cause of the high ^{14}C-CH_4 values.

Further validation of the analytical procedures was conducted by processing standard radiogenically "dead" CH_4 gas through the laboratory procedures, which would reveal if an anomalously high radiocarbon blank was present. In total, we conducted 13 standards tests and the ^{14}C-CH_4 values were ~0 pMC ($-997 \pm 2‰$) (Table 1 and Supplementary Table S2). Moreover, any vacuum line leaks were investigated at the end of the laboratory purification procedures by measuring the increase in the static vacuum pressure as a function of time, which was always under 0.001 Torr/min (Sparrow and Kessler, 2017). Thus, given the validation tests of the field and laboratory procedures, the elevated values of ^{14}C-CH_4 measured are clearly not derived from the analytical techniques employed in this study.

3.1.2. In-situ production of $^{14}CH_4$

Incorporation of naturally produced ^{14}C into a CH_4 molecule is less likely to contribute to the anomalous ^{14}C-CH_4 values. ^{14}C is naturally produced by the nuclear irradiation of N and O by neutrons of cosmic

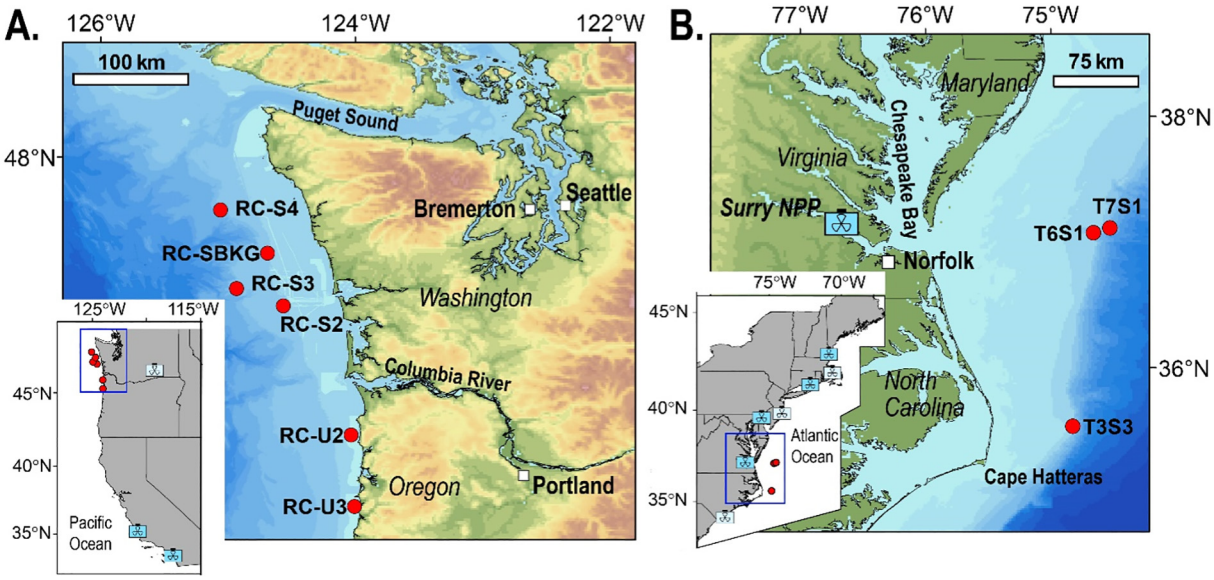

Fig. 2. Locations of sample sites at which anomalously high ^{14}C-CH_4 was observed are shown as red circles. (A) The U.S. Pacific margin samples were collected in 2019, and there were no active nuclear power plants (NPP) in the immediate area. The blue box in the inset map corresponds to the enlarged map. Pale blue NPP symbols on the inset map show boiling water reactors (BWR), and darker blue symbols correspond to pressurized water reactors (PWR). (B) U.S. Atlantic margin data were acquired in 2017, and the Surry NPP, a PWR reactor, is west of Norfolk. The inset map shows coastal NPP that were active in 2017. The PWR symbol is shown if at least one reactor at a particular NPP was a PWR. (For interpretation of the references to colour in this figure legend, the reader is referred to the web version of this article.)

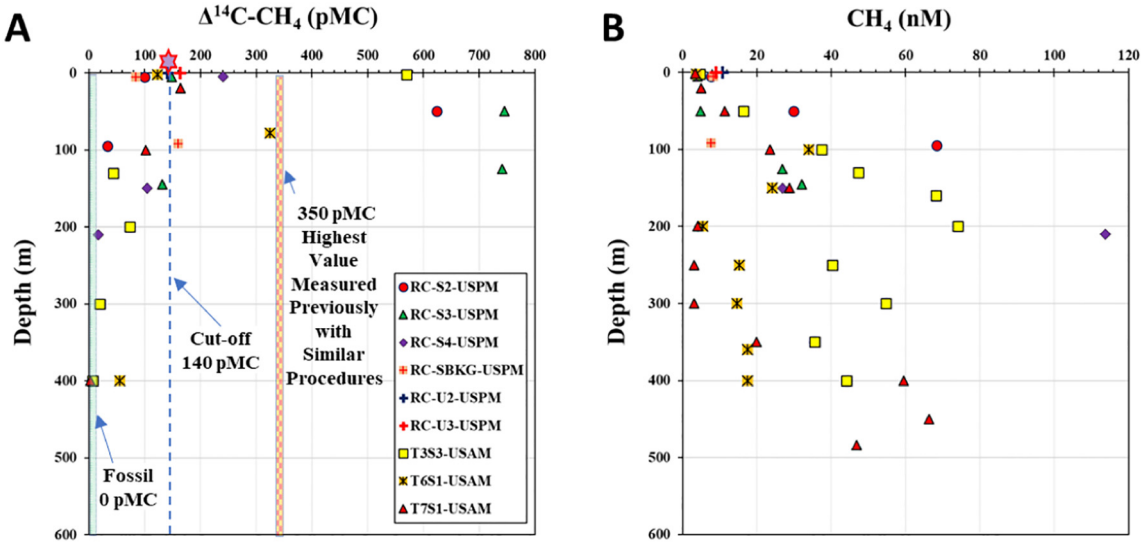

Fig. 3. Vertical distributions of a) ^{14}C-CH$_4$ (pMC) and b) CH$_4$ concentrations at both US-Pacific and US-Atlantic Margin sites. A star in a) represents the contemporary atmospheric value of ^{14}C-CH$_4$, ~ 135 pMC. The 350 pMC cutoff value was chosen since it was the highest value observed previously in ocean water near the Santa Barbara Basin (23).

rays in the atmosphere, surface waters, and ice (Yim and Caron, 2006; Ma and Von Hippel, 2001). The current atmospheric and biotic mass activities of ^{14}C (not ^{14}C-CH$_4$) in environments are expected to be ~250 Bq/kg-C (i.e. ~117 pMC, Bq: = disintegration per second), which decreased after the prohibition of atmospheric nuclear bomb tests and is close to the levels prior to such anthropogenic activities (Yim and Caron, 2006; Lal and Jull, 1990). Kessler et al. (2008) examined the possible introduction of naturally produced ^{14}C to ocean waters and its incorporation into the CH$_4$ molecule. In these previous analyses, the atmospheric introduction and in situ production of ^{14}CO and ^{14}CO$_2$ in ocean waters were viewed as precursors that were subsequently reduced to ^{14}CH$_4$. Kessler et al. (2008) considered the possibility that ^{14}CO formed in the atmosphere dissolves into seawater and is fully reduced to ^{14}CH$_4$. They estimated that this process only contributes at most 2.8% to observed values of ^{14}C-CH$_4$. Kessler et al. (2008) also calculated that the in-situ production rate of ^{14}CH$_4$ in seawater could be as high as 1.1×10^{-15} nmol L^{-1} per day, which is at most 6.9% of the value necessary to balance sinks via oxidation. ^{14}CO$_2$ can also diffuse into the ocean surface and be reduced to ^{14}CH$_4$. However, ^{14}CO$_2$ is immediately diluted with dissolved inorganic carbon (DIC) in seawater, and DIC radiocarbon has not been reported to be greater than what can be attributable to the atmospheric testing of nuclear weapons (Kessler et al., 2008). Thus, Kessler et al. (2008) concluded that no mechanism of natural ^{14}C production and its incorporation into CH$_4$ was able to generate the elevated values found in their study. Moreover, this natural production cannot explain the variations between locations and at different water depths in the same location, as described here and in our previous studies (Kessler et al., 2008; Sparrow et al., 2018; Joung et al., 2019).

3.1.3. Natural methanogenesis or isotopic fractionation in seawater

The highly elevated values reported here (>140 pMC) were unlikely to have originated from the contemporary atmosphere or any natural process. (1) Contemporary ^{14}C-CH$_4$ in the atmosphere is known to be approximately 135 pMC, though variations in both time and space have been observed (Wahlen et al., 1989; Lassey et al., 2007; Townsend-Small et al., 2012; Graven et al., 2019). For ocean surface waters in equilibrium with the atmosphere, ocean ^{14}C-CH$_4$ values should be similar to those in the atmosphere because the dissolution isotopic fractionation factor between the atmosphere and water is small ($\alpha \approx 1.00033$; Fuex, 1980). (2) The ^{14}C-CH$_4$ values we discuss here are not influenced by oxidation isotopic fractionation since they are normalized to ^{13}C (Stuiver and Polach, 1977). The elevated pMC values therefore cannot be an artifact of biological CH$_4$ oxidation. Similarly, this normalization eliminates any small isotopic fractionation in the air-sea equilibrium. (3) Methane produced in waters and sediments, either anaerobically or aerobically, should have values below 110 pMC since precursors for CH$_4$ production have values below this limit. For example, dissolved inorganic carbon in surface seawater has ^{14}C values of approximately 100 to 110 pMC (or 0–100‰) (Beaupré and Aluwihare, 2010; Toggweiler et al., 2019). Also, organic matter in waters and surficial sediments in the northeast Pacific Ocean has lower ^{14}C values (44 pMC or ca. −560‰) (Druffel et al., 2019). This indicates that the ^{14}C signatures of CH$_4$ produced in ocean waters and sediments would have values equal to or less than these precursors, far different from the observed anomalies.

3.2. Likely cause of anomalous values of ^{14}C-CH$_4$: contamination of seawater by nuclear power

Anthropogenic contamination of ^{14}C-CH$_4$ is not likely to originate from local laboratory equipment or sample handling but could be sourced regionally from nuclear power infrastructure. NPPs have been recognized as a significant source of the ^{14}CH$_4$ isotopologue (Eisma et al., 1994; Lassey et al., 2007; Kessler et al., 2008; Townsend-Small et al., 2012). Eisma et al. (1994, 1995) reported 467 pMC of ^{14}C-CH$_4$ in the atmosphere near a NPP in the Netherlands. In the water column, greater than contemporary values have also been reported (e.g., Kessler et al., 2008; Joung et al., 2019, 2020), which are likely associated with NPPs near their sample collection sites. For example, Kessler et al. (2008) and Joung et al. (2020) observed ~350 pMC and ~163 pMC, respectively, of ^{14}C-CH$_4$ in Santa Barbara Basin and explained that these high values likely originated from effluents of the Diablo Canyon NPP, which uses ocean water for cooling. Joung et al. (2019) found elevated ^{14}C-CH$_4$ (~145 pMC) in Lake Michigan, where multiple pressurized-water NPPs along the shore use lake water for cooling. Thus, while observing values of ^{14}C-CH$_4$ > 135 pMC is uncommon, it is not unusual in natural waters when point sources related to nuclear power generation are nearby.

In this study, both the USAM and USPM sampling sites are too distant from land-based NPPs for these plants to be the source of the high pMC ^{14}C-CH$_4$ anomalies (Fig. 2). For the USPM sites with elevated ^{14}C-CH$_4$ values, the nearest active NPP is ~1500 km away at Diablo Canyon on the central California coast. We also investigated if the high

^{14}C-CH_4 along the USPM was related to the Fukushima Daichi NPP incident. However, this NPP is a boiling water type reactor, which mostly produces gaseous CO_2 (Graven et al., 2019). Furthermore, Povinec et al. (2017) found only a 6–7% increase of ^{14}C in oceanic DIC (98.5 pMC to 99.3 pMC or −115‰ to ca. −107‰) relative to background waters near the Fukushima incident site. In the USAM, the T3S3 station is about 270 km away from the nearest land-based, pressurized-water NPP, located at Surry Power Station, VA. Any effluents released in the cooling water would have to navigate the James River and Chesapeake Bay before entering the coastal USAM, with possible additional dilution from the Gulf Stream, Labrador Cold current, and local variations from tides and winds (Fredj et al., 2016). Thus, while some NPPs release effluents with ^{14}C-CH_4 characteristics consistent with those in our elevated samples, land-based NPPs cannot explain the characteristics and distribution of all elevated samples in our dataset.

In the ocean, vessels (e.g., ships and submarines) powered by pressurized water nuclear reactors (PWRs) provide another source of anthropogenic $^{14}CH_4$ production. At present, there are approximately 150 nuclear-powered vessels (mostly for military use) with more than 220 reactors (Namikawa et al., 2011). As of October 2019, the US Navy (USN) alone runs 79 active nuclear-powered ships with 98 reactors (Naval Reactors Annual Reports, 2020a). With each reactor producing ~200 MW (M = 10^6 W = annual electricity production in Watts) (Namikawa et al., 2011), a total worldwide energy output of 44 GW (G = 10^9) is estimated for nuclear-powered vessels if all reactors were active simultaneously.

Determining how NPPs affect ^{14}C-CH_4 in the environment is challenging because emission rates and endmember values of ^{14}C-CH_4 produced by NPPs have not been systematically measured and openly reported with regional and temporal detail. However, Eisma et al. (1995) modeled the production of ^{14}C from PWRs to be 260 ± 50 GBq/GW. Zazzeri et al. (2018) reported strong variability of the emission factor, spanning values from 30 to 2520 GBq/GW. Both Eisma et al. (1995) and Zazzeri et al. (2018) suggested that about 72% of ^{14}C from PWRs is in the form of CH_4. Taking Eisma's estimation of ^{14}C production from NPP (260 GBq/GW) and the power generated by all the nuclear vessels (44 GW), the maximum production of $^{14}CH_4$ by nuclear vessels can be crudely estimated to be 8200 GBq (=260 GBq/GW × 44 GW × 0.72) or 3.6 mol (=8200 GBq/(Avogadro's Number × 0.693/half-life in seconds)) of $^{14}CH_4$ per year. This mass is undetectable in terms of concentration when diluted throughout the global ocean with a standing stock of CH_4 of 43.2 Tg (Reeburgh, 2007). However, since the isotopic abundance of ^{14}C relative to ^{12}C in a modern sample is roughly 1 part in 10^{12}, this isotopic signature could be detectable globally if not removed by oxidation or atmospheric emission.

A single nuclear-powered vessel can generate electrical output of ~0.20 GW (Namikawa et al., 2011), but has variations based on its model and type (Naval Reactors Annual Reports, 2020a). This output leads to the production of approximately 37.4 GBq or 16 mmol of $^{14}CH_4$ per year. Assuming a vessel speed of 27 km/h (15 knots), only 2.2 min are needed for a nuclear-powered vessel to pass through one of our sampling sites, assuming the maximum drift of our vessel during sample collection is 1 km. We further assume during normal cruising conditions that a nuclear-powered vessel uses the power of only a quarter of the reactor's maximum output (Naval Reactors Annual Reports, 2020a). Thus, during the 2.2-min transit, a nuclear-powered vessel could produce ~17 nmol (7.7 nmol/min × 2.2 min) of $^{14}CH_4$ across our sampling location. Considering that the amount of water filtered for our sampling process can be more than 30,000 L (Table 1), the CH_4 addition from the nuclear-powered vessel accounts for ca. 0.01% of the CH_4 mass collected, assuming a dissolved CH_4 concentration of 4.6 nM, as found in the surface waters at station T3S3 along the USAM. This calculation is an upper estimate as it ignores waters with higher background concentrations of dissolved CH_4 and assumes that all emissions from the nuclear-powered vessel in the 2.2 min required to pass through our collection area are captured by our procedures rather than being partially dispersed. Nonetheless, this estimate yields a minimal influence on the dissolved CH_4 concentration, while also suggesting the potential for noticeable influence on the natural radiocarbon abundance.

Contemporary atmospheric ^{14}C-CH_4 has a value 135 pMC, leading to the specific activity of 289 Bq/kg-C (at −47‰ of $\delta^{13}C$-CH_4 in atmosphere; Milkov et al., 2020) (see, Supplementary Materials for calculation). The approximate carbon mass from CH_4 that we collected in surface water sites was 1.7 mg (30,000 L of seawater, 1.025 kg/L of seawater, and ~4.6 nM of CH_4 in surface seawater at station T3S3). Thus, the surface water samples would yield about 0.0005 Bq in CH_4 carbon assuming they are in equilibrium with the atmosphere.

In contrast, a nuclear vessel with a single reactor operating at ~25% of the full power output can generate 39.6 KBq of ^{14}C (17.1 nmol in 2.2 min, =17.1 × 10^{-9} × Avogadro's Number × ^{14}C-decay constant in second), which is about 8.1 × 10^7 times greater than what is expected in surface water without this anthropogenic source. This means that even an extreme dilution ratio of 1: ~20,000,000 would still increase the ^{14}C-CH_4 from 135 pMC to 700 pMC (Fig. 4). This calculation illustrates that nuclear-powered vessels can significantly alter the ^{14}C

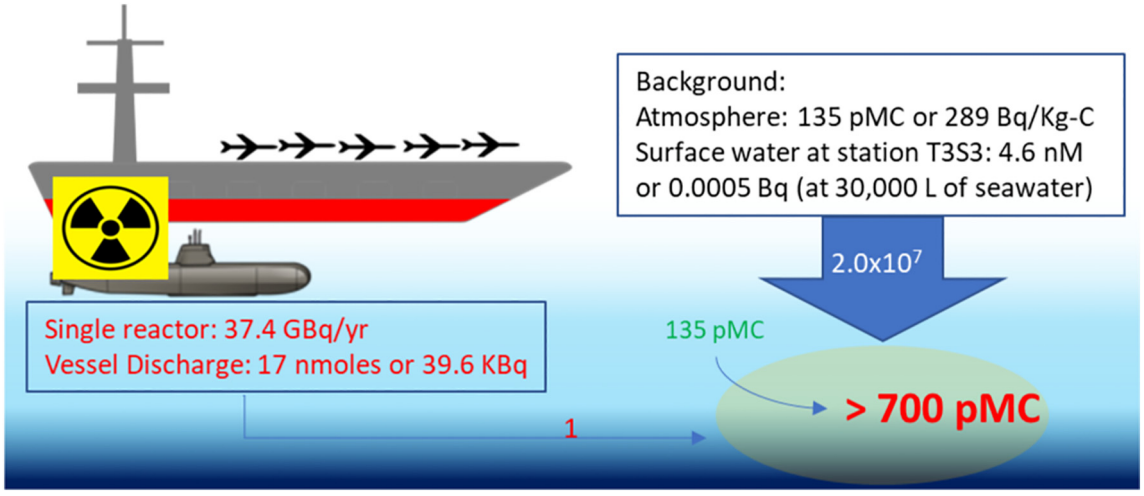

Fig. 4. Schematic diagram illustrating the significant impact that nuclear-powered vessels have on ^{14}C-CH_4 signals in seawater. Even under the extreme mixing scenario where the discharge from nuclear-powered vessels is diluted by a ratio of 1: 2.0 × 10^7, the ^{14}C-CH_4 signal in surface seawater increases from 135 to >700 pMC. This calculation assumes that the vessel runs at 25% of the maximum energy output and that discharge from the nuclear vessel occurring across 1 km intersected with the sample collection efforts described here. Thus, across this 1 km with a vessel speed of 27 km/h (15 knots), the nuclear-powered vessel takes 2.2 min to pass our sample collection site, releasing about 17 nmole or 39.6 KBq of $^{14}CH_4$. At the ocean surface where the ^{14}C-CH_4 is in equilibrium with atmosphere, the total ^{14}C activity is 0.0005 Bq.

isotopic values in CH_4 without notable increases in the local-scale concentration of CH_4. In addition, this rough estimate suggests that sampling even a small fraction of CH_4 released from nuclear-powered vessels to the oceanic environment would considerably alter the natural ^{14}C-CH_4 signal. Since nuclear-powered vessels have more than one reactor, this single-reactor based estimate might be a lower bound for the influence of CH_4 produced by passage of a nuclear-powered vessel.

Although the elevated ^{14}C-CH_4 signals we measure in some seawaters were likely derived from nuclear-powered vessels, it is still unclear how the $^{14}CH_4$ contamination is introduced to the seawater. Possible explanations include seawater reactions involving neutrons leaked from the vessel or discharge of coolant used for reducing extra heat from the nuclear reactors. We consider the first possibility to be unlikely since any leaked neutrons would likely interact with chemical elements having strong neutron reaction thermal cross sections and high concentrations (e.g., B with 3800 b and ~5 mg/kg; Sears, 1992; Lee et al., 2010) before encountering ^{15}N (=0.000024 b) or with other ^{14}C parents. Even if ^{14}C is produced in this way, it would likely be converted to ^{14}CO and $^{14}CO_2$ rather than $^{14}CH_4$ due to the abundance of dissolved O_2 in seawater. Thus, any leaked neutrons likely do not contribute to elevated ^{14}C-CH_4 in seawater (Supplementary Materials).

In contrast, the USN reports (Naval Reactors Annual Reports, 2020b) that a vessel's release of coolant waters containing long-lived radionuclides often occurs close to a Navy base at a distance within ~20 km (12 miles) from the shore and that the total activities in released liquids are typically <0.4 Ci (1.48×10^{10} Bq; total long-lived gamma radioactivity) per year and <100 Ci release of ^{14}C per year. While this value is much less than annual natural production (c.f., 40,000 Ci of ^{14}C per year, Naval Reactors Annual Reports, 2020b), the local and short-duration nature of coolant release means that this anthropogenic signal could be detectable in our measurements. As discussed above, only small fractions of the discharged $^{14}CH_4$ are needed to cause elevated ^{14}C-CH_4 values. Thus, although only very low levels of radioactive methane are released from the vessel, the signal can be detectable when the discharged liquids are not fully mixed regionally, which may be the case in certain areas of the USAM and USPM.

Some other sites on both the USAM (T6S1, T7S1) and USPM (RC-S4, -BKG, —U2, and —U3) have also shown elevated ^{14}C-CH_4 relative to the contemporary atmosphere, but at magnitudes much less than RC-S2 and-S3. Again, the areas we studied were not close to active NPPs. Thus, these additional anomalously high ^{14}C-CH_4 values were also likely derived from nuclear-powered vessels, although dispersion, atmospheric emission, and possibly oxidation of this discharge may have reduced the influence of this source.

The explanations provided here for the observed ^{14}C-CH_4 anomalies are based on no knowledge of the tracks of nuclear-powered vessels through our sampling sites. However, many of these sampling locations are near well-known USN ports such as Norfolk, Virginia and Seattle, Washington. Our results thus suggest that waters near nuclear powered activities— both power plants and vessels that use pressurized water reactors— can lead to discharge of $^{14}CH_4$ causing anomalously high pMC values. Further systematic study in the vicinity of nuclear-powered vessels operating under normal conditions would be necessary to confirm source attribution and assess environmental impacts. Regardless, such contamination can significantly influence and confuse the interpretation of natural ^{14}C-CH_4 measurements in ocean waters. This discovery further highlights the potential to use such measurements to track the general positions of nuclear-powered vessels.

4. Conclusion

With growing attention to and utilization of ^{14}C analysis for attribution studies of natural CH_4 sources, a full understanding of anthropogenic sources of $^{14}CH_4$ and how they might influence the interpretation of measured values is critical. Pressurized-water nuclear reactors have previously been established as sources of $^{14}CH_4$, and some coastal waters near these types of NPPs have shown elevated ^{14}C-CH_4 signals. However, we found that some marine waters at sites distant from the land-based NPPs also have ^{14}C-CH_4 values elevated by at least 4–5 times higher than the contemporary surface ocean's ^{14}C-CH_4. Our calculations strongly suggest that these localized, very high ^{14}C-CH_4 values reflect the influence of nuclear-powered vessels discharging $^{14}CH_4$. While this is the most plausible explanation, we have no knowledge of the specific amount of $^{14}CH_4$ discharge in our study areas, nor the tracks of the nuclear-powered vessels. Nonetheless, our measurements and calculations show that these emissions can significantly affect the natural radiocarbon abundances on local scales. Thus, when choosing sample collection sites and interpreting the results of ^{14}C-CH_4, these potential anthropogenic sources should be considered.

CRediT authorship contribution statement

D.J.J., C.R., and J.D·K. designed the study, and J.S. measured ^{14}C-CH_4 using the accelerator mass spectrometry (AMS). D.J.J. and J.D.K collected and prepared samples in the field and laboratory. All authors equally contributed to the interpretation of the data and writing of this manuscript.

Funding sources

This research was funded by grants to J.K. from NSF (OCE-1851402, OCE-1634871, and PLR-1417149) and DOE (DE-FE0028980). C.R. was supported by USGS-DOE Interagency Agreements (DE-FE0026195 and 89243320SFE000013).

Declaration of competing interest

The authors declare that they have no known competing financial interests or personal relationships that could have appeared to influence the work reported in this paper.

Contact and competing interest information for all authors.

The authors declare no competing financial interest.

All data in this manuscript is available to the scientific community through the BCO-DMO database. Kessler, J. D., Joung, D. (2021) Radiocarbon in methane from waters of the US Atlantic and Pacific margins as collected on R/V Hugh Sharp cruise HRS1713 and R/V Rachel Carson cruise RC0026 in 2017 and 2019, respectively. Biological and Chemical Oceanography Data Management Office (BCO-DMO). (Version 1) Version Date 2021-09-27. doi:https://doi.org/10.26008/1912/bco-dmo.861576.1

Acknowledgments

We acknowledge the outstanding technical support we received from crew members of the R/V Hugh R. Sharp and the R/V Rachel Carlson. Any use of trade, firm or product name is for descriptive purposes only and does not imply endorsement by the U.S. Government.

Appendix A. Supplementary data

Supporting information includes further details about the data sets, sample collection in the field, and the preparation of the collected samples in the land-based laboratory, estimation of ^{14}C activity in the sample (conversion from pMC to activity), neutron reactions in seawater and ocean release of liquids from nuclear-powered vessels, and other techniques for ^{14}C activity measurement in the sample. The results of the purification system tests and the analysis of the samples can also be found in the Supporting Information (Joung et al. 2021-STOTEN Supplementary Materials). Supplementary data to this article can be found online at doi:https://doi.org/10.1016/j.scitotenv.2021.150456.

References

Anthony, K.M.W., Anthony, P., Grosse, G., Chanton, J., 2012. Geologic methane seeps along boundaries of Arctic permafrost thaw and melting glaciers. Nat. Geosci. 5 (6), 419–426.

Beaupré, S.R., Aluwihare, L., 2010. Constraining the 2-component model of marine dissolved organic radiocarbon. Deep-Sea Res. II Top. Stud. Oceanogr. 57 (16), 1494–1503.

Brandt, A.R., Heath, G., Kort, E., O'Sullivan, F., Pétron, G., Jordaan, S.M., Tans, P., Wilcox, J., Gopstein, A., Arent, D., 2014. Methane leaks from North American natural gas systems. Science 343 (6172), 733–735.

Bruhwiler, L., Basu, S., Bergamaschi, P., Bousquet, P., Dlugokencky, E., Houweling, S., Ishizawa, M., Kim, H.S., Locatelli, R., Maksyutov, S., 2017. US CH4 emissions from oil and gas production: have recent large increases been detected? J. Geophys. Res. Atmos. 122 (7), 4070–4083.

Douglas, P., Stolper, D., Smith, D., Anthony, K.W., Paull, C., Dallimore, S., Wik, M., Crill, P.M., Winterdahl, M., Eiler, J., 2016. Diverse origins of Arctic and subarctic methane point source emissions identified with multiply-substituted isotopologues. Geochim. Cosmochim. Acta 188, 163–188.

Druffel, E.R., Griffin, S., Wang, N., Garcia, N.G., McNichol, A.P., Key, R.M., Walker, B.D., 2019. Dissolved organic radiocarbon in the Central Pacific Ocean. Geophys. Res. Lett. 46 (10), 5396–5403.

Eisma, R., Van der Borg, K., De Jong, A., Kieskamp, W., Veltkamp, A., 1994. Measurements of the 14C content of atmospheric methane in the Netherlands to determine the regional emissions of 14CH4. Nucl. Instrum. Methods Phys. Res., Sect. B 92 (1–4), 410–412.

Eisma, R., Vermeulen, A.T., Van Der Borg, K., 1995. 14CH4 emissions from nuclear power plants in northwestern Europe. Radiocarbon 37 (2), 475–483.

Fredj, E., Roarty, H., Kohut, J., Smith, M., Glenn, S., 2016. Gap filling of the coastal ocean surface currents from HFR data: application to the mid-Atlantic bight HFR network. J. Atmos. Ocean. Technol. 33 (6), 1097–1111.

Fuex, A., 1980. Experimental evidence against an appreciable isotopic fractionation of methane during migration. Phys. Chem. Earth 12, 725–732.

Graven, H.D., 2015. Impact of fossil fuel emissions on atmospheric radiocarbon and various applications of radiocarbon over this century. Proc. Natl. Acad. Sci. 112 (31), 9542–9545.

Graven, H., Hocking, T., Zazzeri, G., 2019. Detection of fossil and biogenic methane at regional scales using atmospheric radiocarbon. Earth's Future 7 (3), 283–299.

Joung, D., Leonte, M., Kessler, J.D., 2019. Methane sources in the waters of Lake Michigan and Lake Superior as revealed by natural radiocarbon measurements. Geophys. Res. Lett. 46 (10), 5436–5444.

Joung, D., Leonte, M., Valentine, D.L., Sparrow, K., Weber, T., Kessler, J.D., 2020. Radiocarbon in marine methane reveals patchy impact of seeps on surface waters. Geophys. Res. Lett. 47 (20), e2020GL089516.

Kessler, J., Reeburgh, W., Southon, J., Varela, R., 2005. Fossil methane source dominates Cariaco Basin water column methane geochemistry. Geophys. Res. Lett. 32 (12).

Kessler, J., Reeburgh, W., Tyler, S., 2006. Controls on methane concentration and stable isotope (δ2H-CH4 and δ13C-CH4) distributions in the water columns of the Black Sea and Cariaco Basin. Glob. Biogeochem. Cycles 20, (4).

Kessler, J., Reeburgh, W., Valentine, D., Kinnaman, F., Peltzer, E., Brewer, P., Southon, J., Tyler, S., 2008. A survey of methane isotope abundance (14C, 13C, 2H) from five nearshore marine basins that reveals unusual radiocarbon levels in subsurface waters. J. Geophys. Res. Oceans 113 (C12).

Kunz, C., 1985. Carbon-14 discharge at three light-water reactors. Health Phys. 49 (1), 25–35.

Lal, D., Jull, A.T., 1990. On determining ice accumulation rates in the past 40,000 years using in situ cosmogenic 14C. Geophys. Res. Lett. 17 (9), 1303–1306.

Lassey, K., Lowe, D., Smith, A., 2007. The atmospheric cycling of radiomethane and the" fossil fraction" of the methane source. Atmos. Chem. Phys. 7 (8), 2141–2149.

Lee, Kitack, Kim, Tae-Wook, Byrne, Robert H., Millero, Frank J., Feely, Richard A., Liu, Yong-Ming, 2010. The universal ratio of boron to chlorinity for the North Pacific and North Atlantic oceans. Geochim. Cosmochim. Acta 74 (6), 1801–1811.

Leonte, M., Kessler, J.D., Kellermann, M.Y., Arrington, E.C., Valentine, D.L., Sylva, S.P., 2017. Rapid rates of aerobic methane oxidation at the feather edge of gas hydrate stability in the waters of Hudson Canyon, US Atlantic Margin. Geochim. Cosmochim. Acta 204, 375–387.

Leonte, M., Wang, B., Socolofsky, S.A., Mau, S., Breier, J.A., Kessler, J.D., 2018. Using carbon isotope fractionation to constrain the extent of methane dissolution into the water column surrounding a natural hydrocarbon gas seep in the northern Gulf of Mexico. Geochem. Geophys. Geosyst. 19 (11), 4459–4475.

Ma, C., Von Hippel, F., 2001. Ending the production of highly enriched uranium for naval reactors. Nonproliferation Rev. 8 (1), 86–101.

Milkov, A.V., Schwietzke, S., Allen, G., Sherwood, O.A., Etiope, G., 2020. Using global isotopic data to constrain the role of shale gas production in recent increases in atmospheric methane. Sci. Rep. 10 (1), 1–7.

Muller, R.A., 2010. Submarines, quarks, and radioisotope dating 1. Radiocarbon 52 (2), 209–218.

Namikawa, S., Mærli, M., Hoffmann, P., Brodin, E., 2011. May. nuclear powered ships–findings from a feasibility study. Proc. 19th Int. Conf. Nuclear Engineering (ICONE19).

Naval Reactors annual reports, 2020a. 2020 United States naval nuclear propulsion program. https://www.energy.gov/nnsa/downloads/naval-reactors-annual-reports. (Accessed 13 July 2021).

Naval Reactors annual reports, 2020b. Environmental monitoring and disposal of radioactive wastes from U.S. naval nuclear-powered ships and their support facilities. https://www.energy.gov/nnsa/downloads/naval-reactors-annual-reports. (Accessed 13 July 2021).

Pack, M.A., Heintz, M.B., Reeburgh, W.S., Trumbore, S.E., Valentine, D.L., Xu, X., Druffel, E.R., 2011. A method for measuring methane oxidation rates using low levels of 14C-labeled methane and accelerator mass spectrometry. Limnol. Oceanogr. Methods 9 (6), 245–260.

Pohlman, J.W., Bauer, J.E., Canuel, E.A., Grabowski, K.S., Knies, D., Mitchell, C., Whiticar, M.J., Coffin, R.B., 2009. Methane sources in gas hydrate-bearing cold seeps: evidence from radiocarbon and stable isotopes. Mar. Chem. 115 (1–2), 102–109.

Povinec, P., Kwong, L.L.W., Kaizer, J., Molnár, M., Nies, H., Palcsu, L., Papp, L., Pham, M.K., Jean-Baptiste, P., 2017. Impact of the Fukushima accident on tritium, radiocarbon and radiocesium levels in seawater of the western North Pacific Ocean: a comparison with pre-Fukushima situation. J. Environ. Radioact. 166, 56–66.

Quay, P., Stutsman, J., Wilbur, D., Snover, A., Dlugokencky, E., Brown, T., 1999. The isotopic composition of atmospheric methane. Glob. Biogeochem. Cycles 13 (2), 445–461.

Reeburgh, W.S., 2007. Oceanic methane biogeochemistry. Chem. Rev. 107 (2), 486–513.

Repeta, D.J., Ferrón, S., Sosa, O.A., Johnson, C.G., Repeta, L.D., Acker, M., DeLong, E.F., Karl, D.M., 2016. Marine methane paradox explained by bacterial degradation of dissolved organic matter. Nat. Geosci. 9 (12), 884–887.

Ruppel, C.D., Kessler, J.D., 2017. The interaction of climate change and methane hydrates. Rev. Geophys. 55 (1), 126–168.

Sapart, C.J., Shakhova, N., Semiletov, I., Jansen, J., Szidat, S., Kosmach, D., Dudarev, O., Van Der Veen, C., Egger, M., Sergienko, V., 2017. The origin of methane in the east siberian Arctic shelf unraveled with triple isotope analysis. Biogeosciences 14 (9), 2283–2292.

Saunois, M., Jackson, R., Bousquet, P., Poulter, B., Canadell, J., 2016. The growing role of methane in anthropogenic climate change. Environ. Res. Lett. 11 (12).

Sears, V.F., 1992. Neutron scattering lengths and cross sections. Neutron News 3 (3), 26–37.

Sparrow, K.J., Kessler, J.D., 2017. Efficient collection and preparation of methane from low concentration waters for natural abundance radiocarbon analysis. Limnol. Oceanogr. Methods 15 (7), 601–617.

Sparrow, K.J., Kessler, J.D., 2018. Comment on "The origin of methane in the East Siberian Arctic Shelf unraveled with triple isotope analysis" by Sapart et al. (2017). Biogeosciences 15, 4777–4779.

Sparrow, K.J., Kessler, J.D., Southon, J.R., Garcia-Tigreros, F., Schreiner, K.M., Ruppel, C.D., Miller, J.B., Lehman, S.J., Xu, X., 2018. Limited contribution of ancient methane to surface waters of the US Beaufort sea shelf. Sci. Adv. 4, eaao4842.

Stuiver, M., Polach, H.A., 1977. Discussion reporting of 14 C data. Radiocarbon 19 (3), 355–363.

Toggweiler, J., Druffel, E.R., Key, R.M., Galbraith, E.D., 2019. Upwelling in the ocean basins north of the ACC: 1. On the upwelling exposed by the surface distribution of Δ14C. J. Geophys.Res. Oceans 124 (4), 2591–2608.

Townsend-Small, A., Tyler, S.C., Pataki, D.E., Xu, X., Christensen, L.E., 2012. Isotopic measurements of atmospheric methane in Los Angeles, California, USA: influence of "fugitive" fossil fuel emissions. J. Geophys. Res. Atmos. 117 (D7).

Wahlen, M., Tanaka, N., Henry, R., Deck, B., Zeglen, J., Vogel, J.S., Southon, J., Shemesh, A., Fairbanks, R., Broecker, W., 1989. Carbon-14 in methane sources and in atmospheric methane: the contribution from fossil carbon. Science 245 (4915), 286–290.

Weinstein, A., Navarrete, L., Ruppel, C., Weber, T.C., Leonte, M., Kellermann, M.Y., Arrington, E.C., Valentine, D.L., Scranton, M.I., Kessler, J.D., 2016. Determining the flux of methane into Hudson canyon at the edge of methane clathrate hydrate stability. Geochem. Geophys. Geosyst. 17 (10), 3882–3892.

Winckler, G., Aeschbach-Hertig, W., Holocher, J., Kipfer, R., Levin, I., Poss, C., Rehder, G., Suess, E., Schlosser, P., 2002. Noble gases and radiocarbon in natural gas hydrates. Geophys. Res. Lett. 29.

Yim, M.-S., Caron, F., 2006. Life cycle and management of carbon-14 from nuclear power generation. Prog. Nuclear Energy 48 (1), 2–36.

Zazzeri, G., Yeomans, E.A., Graven, H., 2018. Global and regional emissions of radiocarbon from nuclear power plants from 1972 to 2016. Radiocarbon 60 (4), 1067–1081.